Theor Chem Acc (2011) 130:909–918
DOI 10.1007/s00214-011-0929-5

REGULAR ARTICLE

A computational study on the relationship between formation and electrolytic dissociation of carbonic acid

Shinichi Yamabe · Nao Kawagishi

Received: 11 October 2010 / Accepted: 17 March 2011 / Published online: 27 April 2011

Abstract Calculations at the B3LYP/6-311+G**, MPW1K/6-311+G**, and MP2/6-311+G** level theory were carried out for the $CO_2 + nH_2O \rightarrow H_2CO_3 + (n - 1)H_2O$ chemical reaction, where n denotes the number of water molecules. For $n = 1$, 2, 3, and 4 water molecules, a concerted path (without intermediates) for the formation of H_2CO_3 was obtained. For $n = 6(3 + 3)$ and $n = 8(4 + 4)$ water molecules, the MPW1K and B3LYP/6-311+G** SCRF = PCM methods resulted in an ion-pair intermediate being formed. Here, +3 or +4 stands for the three or four catalytic water molecules. The catalytic water molecules are distinguished from the reaction participating ones (either three or four). For $n = 3 + 5$ and $n = 3 + 10$, two ion-pair intermediates were obtained using both the B3LYP and MPW1K DFT methods. In order to check the method and model dependence, furthermore, $n = 3 + 17$ and $n = 3 + 27$ reacting systems were examined. Here, a likely mechanism of formation and electrolytic dissociation of carbonic acid was found. First, the O_2C–OH_2 complex is formed. Second, it is isomerized to the Zundel cation $H_5O_2^+$. Third, the cation is converted to the carbonic acid. The isomerization, i.e., proton transfer, was computed to occur along the hydrogen-bonded network of the pentagon shape.

Keywords DFT calculations · Ion pair · Zundel cation · Hydrogen bond · Proton transfer · Transition state

1 Introduction

Carbonic acid HO–C(=O)–OH is known to be formed in the reaction between carbon dioxide and water. The association equilibrium constant is 1.7×10^{-3} mol/L at 25 °C (Scheme 1a) [1]. Carbonic acid is a weak acid and its electrolytic dissociation constants K_I and K_{II} are small (Scheme 1b) [2]. The primary question of whether the association occurs after or occurs during the H_2CO_3 formation remains unresolved (Scheme S1).

Many theoretical studies on the reaction, $CO_2 + nH_2O \rightarrow H_2CO_3 + (n - 1)H_2O$, have been carried out [3–10]. Here, n is the number of water molecules and the largest number to date has been 4. The result reported in Ref. [7] is illustrated in Scheme 2. For $n = 4$, the gas-phase RHF/6-31G** calculation was reported to give a transition state (TS or ts) geometry for the concerted proton transfer involving four water molecules. On the other hand, the Onsager model reaction field (SCRF = dipole) RHF/6-31G** calculation was reported to give a TS structure for the $n = 3 + 1$, where $n = 3 + 1$ means that three water molecules are involved in the concerted proton transfer catalyzed by one water molecule. Thus, for $n = 1$, 2, 3, and 4, ion-pair intermediates corresponding to the electrolytic dissociation were not clear for all the calculations made up to now.

Investigation of the effect of the solvent on the structure and various spectra of amino acids and peptides has shown

Dedicated to Professor Akira Imamura on the occasion of his 77th birthday and published as part of the Imamura Festschrift Issue.

Electronic supplementary material The online version of this article (doi:10.1007/s00214-011-0929-5) contains supplementary material, which is available to authorized users.

S. Yamabe (✉) · N. Kawagishi
Department of Chemistry,
Nara University of Education,
Takabatake-cho, Nara 630-8528, Japan
e-mail: yamabes@nara-edu.ac.jp

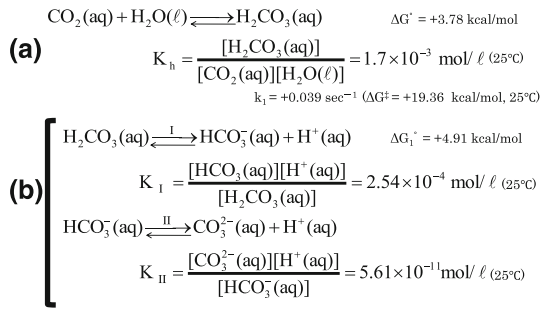

Scheme 1 Two well-known characteristics of carbonic acid, its formation and electrolytic dissociation. Equilibrium and rate constants are experimental data. Ref. [1, 2]

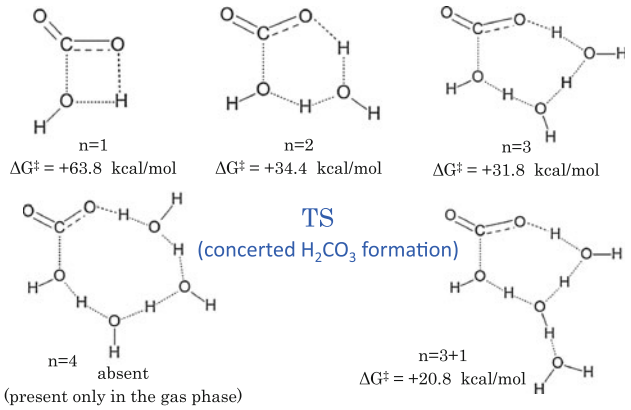

Scheme 2 TS geometries for the concerted reaction, $CO_2 + nH_2O \rightarrow H_2CO_3 + (n-1)H_2O$, obtained by RHF/6-31G** SCRF = dipole optimizations. Activation free energies are relative to the energies of reactant complexes. Ref. [7]

that one needs to treat the solvent using explicit solvent models, and that either isolated state (gas-phase) calculations which do not include the solvent or even continuum solvent models which treat the solvent molecules only implicitly are not adequate [11–27]. In particular, Degtyarenko and coworkers showed that 20 water molecules are necessary to completely solvate the L-alanine zwitterion [25]. Thus, more than 20 water molecules are probably required to examine the $CO_2 + H_2O$ reaction in aqueous solution reliably. In a strongly interacting solvent like water, there are many possible local minima. Depending on the temperature, some of these may be stable, while others are very transient on the potential energy surface. In spite of the complexity, the dominant bond interchange will follow the hydrogen-bond directionality.

In this work, the reaction of $CO_2 + nH_2O \rightarrow H_2CO_3 + (n-1)H_2O$ was investigated systematically with $n = 1$, 2, 3, 4, 8, 13, 20, and 30. When the number of n increases, a clear pattern of proton transfers involving the ion-pair intermediates (int and INT) has been revealed. The abbreviation, int, is used for models of $n = 8$ and 13, and INT for those of $n = 20$ and 30.

2 Method of calculations

The reacting systems were investigated by density functional theory calculations, and the Becke's three-parameter hybrid exchange correlation functional (B3LYP) [28, 29] and the modified Perdew–Wang 1-parameter method for

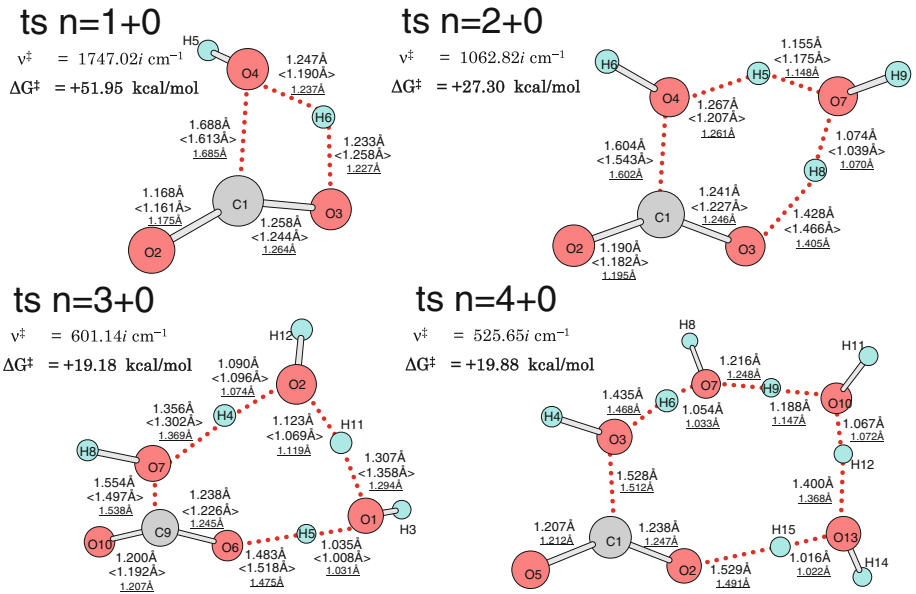

Fig. 1 The ts geometries optimized with B3LYP/6-311+G**, <MPW1K/6-311+G**>, and MP2/6-311+G** for the reaction, $CO_2 + nH_2O \rightarrow H_2CO_3 + (n-1)H_2O$. The calculated activation free energies($\Delta G^\ddagger$s) and the sole imaginary frequencies($\nu^\ddagger$s) are also shown. *Red dotted lines* stand for bond interchange regions (formation or scission)

kinetics (MPW1K) [30] method were used. It is known that the B3LYP method sometimes underestimates barriers for proton-transfer reactions [31]. For this reason, we performed additional geometry optimizations using the hybrid exchange–correlation potential MPW1K, which was parameterized to reproduce barrier heights for chemical reactions. Also, the second-order Moeller-plesset perturbation correlation (MP2) method [32] was used. Geometry optimizations were carried out at the B3LYP/6-311+G**, MPW1K/6-311+G**, and MP2/6-311+G** levels of theory.

Transition states (ts' or TSs) were sought first by partial optimizations at proton-transfer regions. Second, by the use of Hessian matrices, (eigenvalue following) TS geometries were optimized. The optimized structures were characterized by vibrational analysis, where one checks whether the Hessian matrix obtained at the optimized structures has a single imaginary frequency ($v^{\ddagger}$). From ts' or TSs, reaction paths were followed using the intrinsic reaction coordinate method [33, 34] to obtain the energy-minimum geometries. Relative Gibbs free energies ΔGs were obtained at the B3LYP/6-311+G** SCRF = PCM [35–37]//B3LYP/

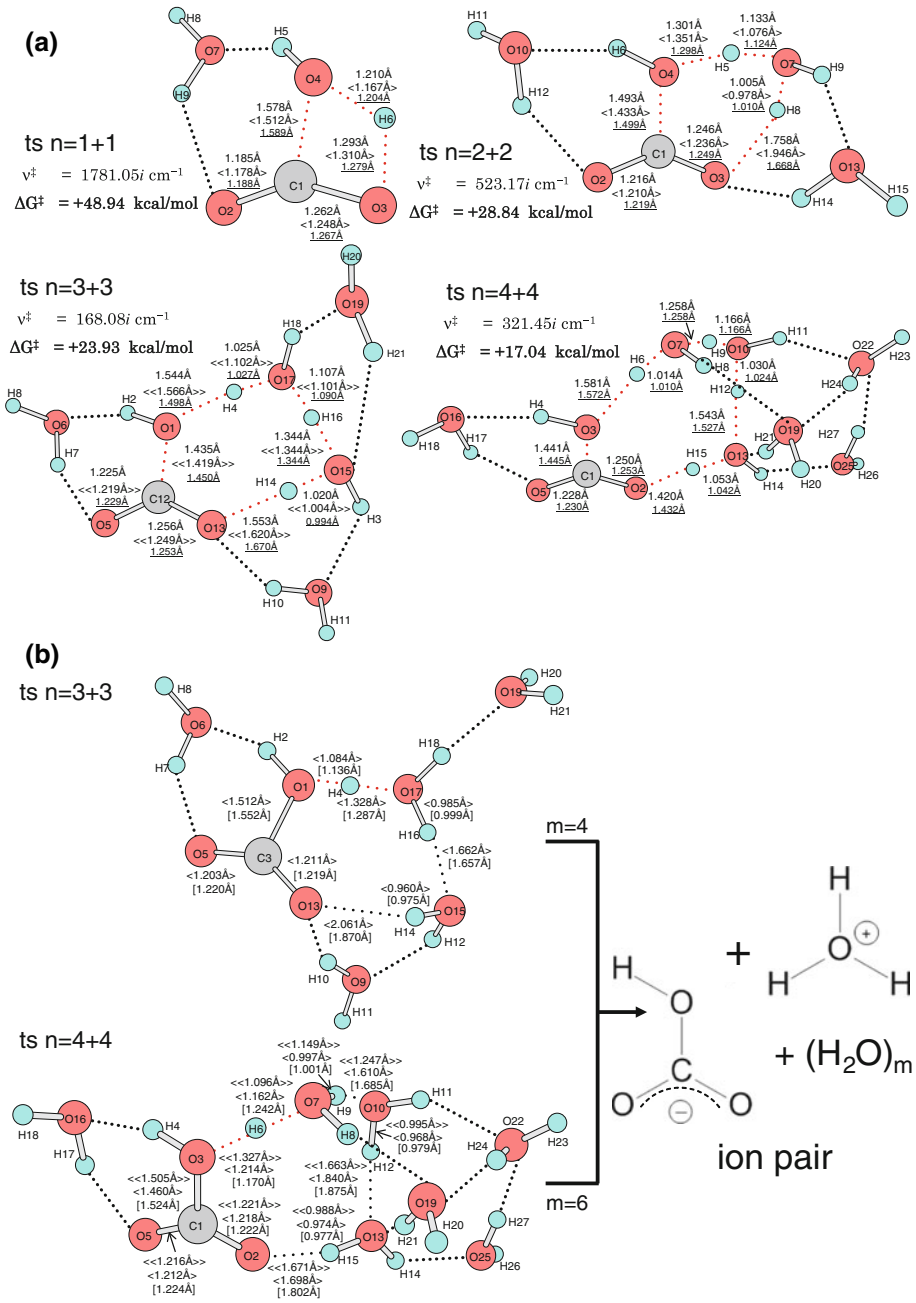

Fig. 2 **a** The ts geometries for the H_2CO_3 formation reaction. Number of catalytic water molecules are shown by +1, +2, +3, and +4. Four reactions were calculated to be concerted. **b** Ts geometries leading to ion-pair intermediates. <MPW1K/6-311+G** gas-phase> and [B3LYP/6-311+G** SCRF = PCM] distances are shown. *m* is the number of water molecules linked with $HOCO_2^-{\cdot}H_3O^+$

6-311+G** level of theory, and thermal corrections ($T = 298.15$ K, $P = 1$ atm) to the Gibbs free energies were included. For smaller models, $n = 1$, 2, 3, 4, 8, and 13, the notation of ts and int was used. For larger ones, $n = 20$ and 30, that of TS and INT was used. For the critical model (the ion pair, present or absent), in Fig. 2, the M06 calculation [38] was also carried out. The lowering of the activation energy by the tunnel effect was estimated by the use of the Wigner's equation ([39], see Supplementary material 2).

A sophisticated method to predict the reaction path was put forth [40]. The method is an extension of the force field–based conformational flooding procedure with an accelerated barrier crossing of chemical reactions (flooding potential). By the method, the ring opening and further rearrangement reactions of two molecules, bicyclopropylidene and methylenecyclopropane, were investigated. Although it is reliable, the present system is too complex for trajectory calculations. Therefore, in this work, the geometry optimizations based on the hydrogen-bond directionality were carried out.

All the calculations were carried out using the GAUSSIAN 09 [41] program package. The computations were performed at the Research Center for Computational Science, Okazaki, Japan.

3 Results and discussions

Figure 1 shows ts geometries for $n = 1$, 2, 3, and 4. Here, the procedure of recomputing the electronic wave function for a changing nuclear geometry was employed to determine the potential energy surface on the basis of the adiabatic, i.e., Born–Oppenheimer approximation. As in the previous studies [3–10], they are for the concerted H_2CO_3 formation. The $n = 1 + 0$ ts, $n = 2 + 0$ ts, $n = 3 + 0$ ts, and $n = 4 + 0$ ts stand for single, double, triple, and quadruple proton transfers, respectively. The $\Delta G^{\ddagger}$ value of $n = 3$ (= +19.18 kcal/mol) is almost the same as that of $n = 4$ (= +19.88 kcal/mol). Next, the effect of catalytic water molecules on the H_2CO_3 formation was examined. The ts geometries of $n = 1 + 1$, $2 + 2$, $3 + 3$, and $4 + 4$ are exhibited in Fig. 2a. For $n = 1 + 1$ and $2 + 2$, B3LYP/6-311+G**, MP2/6-311+G**, and <MPW1K/6-311+G**> gave similar ts geometries. On the other hand, for $n = 3 + 3$ and $n = 4 + 4$, the <MPW1K/6-311+G**> calculations led to different results different from those of B3LYP/6-311+G** and MP2/6-311+G**. The former ts geometries are shown in Fig. 2b, which lead to ion-pair intermediates. B3LYP/6-311+G** SCRF = PCM ts was also found to lead to them.

In Fig. 2a, apparently, ts of $n = 4 + 4$ has the smallest $\Delta G^{\ddagger}$ value (= +17.04 kcal/mol). Therefore, as an extended model, the $n = 4 + 13$ reaction was examined. In spite of many attempts, the H_2CO_3 formation path could not be obtained. Alternatively, as shown in Fig. 3, only an isomerization ts between two ion pairs was found. The absence of the $n = 4$ based model is consistent with the result shown in Scheme 2. The gas-phase $n = 4$ TS geometry was reported to be transformed to the $n = 3 + 1$ one by the SCRF = dipole effect [7]. Hereafter, the $n = 3$ based models were investigated. The way of constructing reaction systems is illustrated in Scheme 3. The $n = 3$ reaction center is surrounded stepwise by outer water molecules for the model expansion, $n = 3 + 3 + 2 + 5 + 7 + 10$. The way of choosing energy-minimum structures in the present system containing many water molecules is explained. First, proton-transfer TS geometries involving the $n = 3$ reaction center and outer hydrogen-bonded water molecules (in Scheme 3) were determined. Second, IRC calculations toward two energy minima located at reverse and forward sides were carried out. Third, geometry

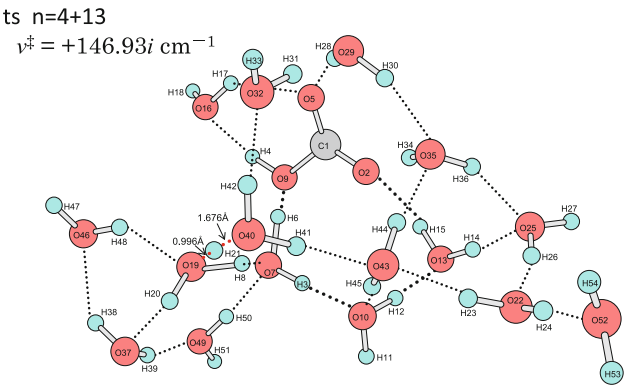

Fig. 3 A ts geometry in the proton-transfer reaction of $CO_2 + (4 + 13)H_2O$, O(19)–H(21)…O(40) → O(19)…H(21)–O(40). The anion moiety HCO_3^- is retained in the reaction

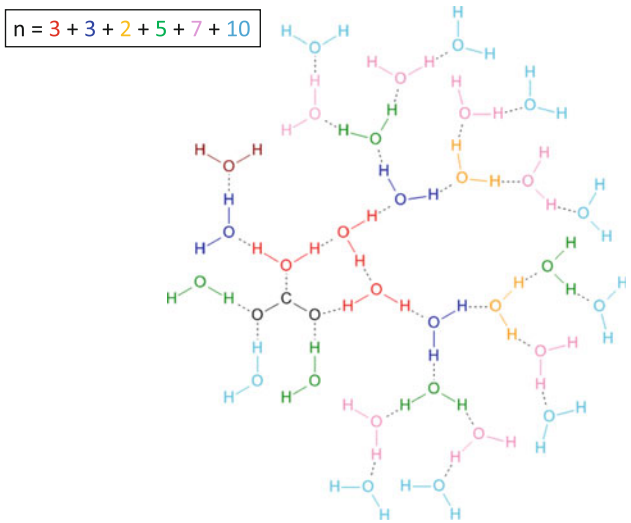

Scheme 3 The $CO_2(H_2O)n$ model employed in this work

optimizations were conducted at the end of IRC calculations to arrive at the energy minimum of $CO_2 + nH_2O$, intermediates, and $H_2CO_3 + (n-1)H_2O$. The local minima on the complicated potential surface were selected on the basis of the $n = 3$ reaction-center moiety. Protons that are not concerned with the central moiety are connected to outer water molecules. The connection obeys the O–H…OH_2 linearity, where the lone-pair orbital of the oxygen atom is directed to the proton. The connection is expanded in the way of Scheme 3, and the assumed geometry was fully optimized.

Figure 4 exhibits reaction paths of $n = 3 + 5$ and $n = 3 + 10$. Results of the two models were found to be similar and are shown together. After the first transition state, ts1, an ion-pair intermediate, int1, is formed. In int1, HCO_3^- and H_3O^+ are involved. The species int1 is isomerized to the second ion-pair intermediate, int2, via ts2. Next, through ts3, int2 is converted to the carbonic acid. The result in Fig. 4 demonstrated that ion pairs which might lead to the electrolytic dissociation are generated during the H_2CO_3 formation. Larger models than $n = 3 + 10$ need to be investigated to check the generation.

Figure 5 shows a reaction of $n = 3 + 17$. When a water molecule is in contact with CO_2 (at TS1), a complex H_2O–CO_2 is formed at INT1. In INT1, a $H_2O \rightarrow CO_2$ coordination bond is involved. INT1 is isomerized to INT2 via TS2. Noteworthy is the geometry of INT2, where the Zundel cation $H_5O_2^+$ [42] is formed with O(10)…H(12) = <1.235 Å> and H(12)…O(25) = <1.388 Å>. The electronic charges displayed in Table S2 also show the character. An INT2–INT3 isomerization takes place at TS3. INT3 is an isomer of the Zundel cation, and INT2 and INT3 are indistinguishable practically. From the cation, the subsequent proton transfer (TS4) leads to the carbonic acid. Figure 5 has indicated two characteristics.

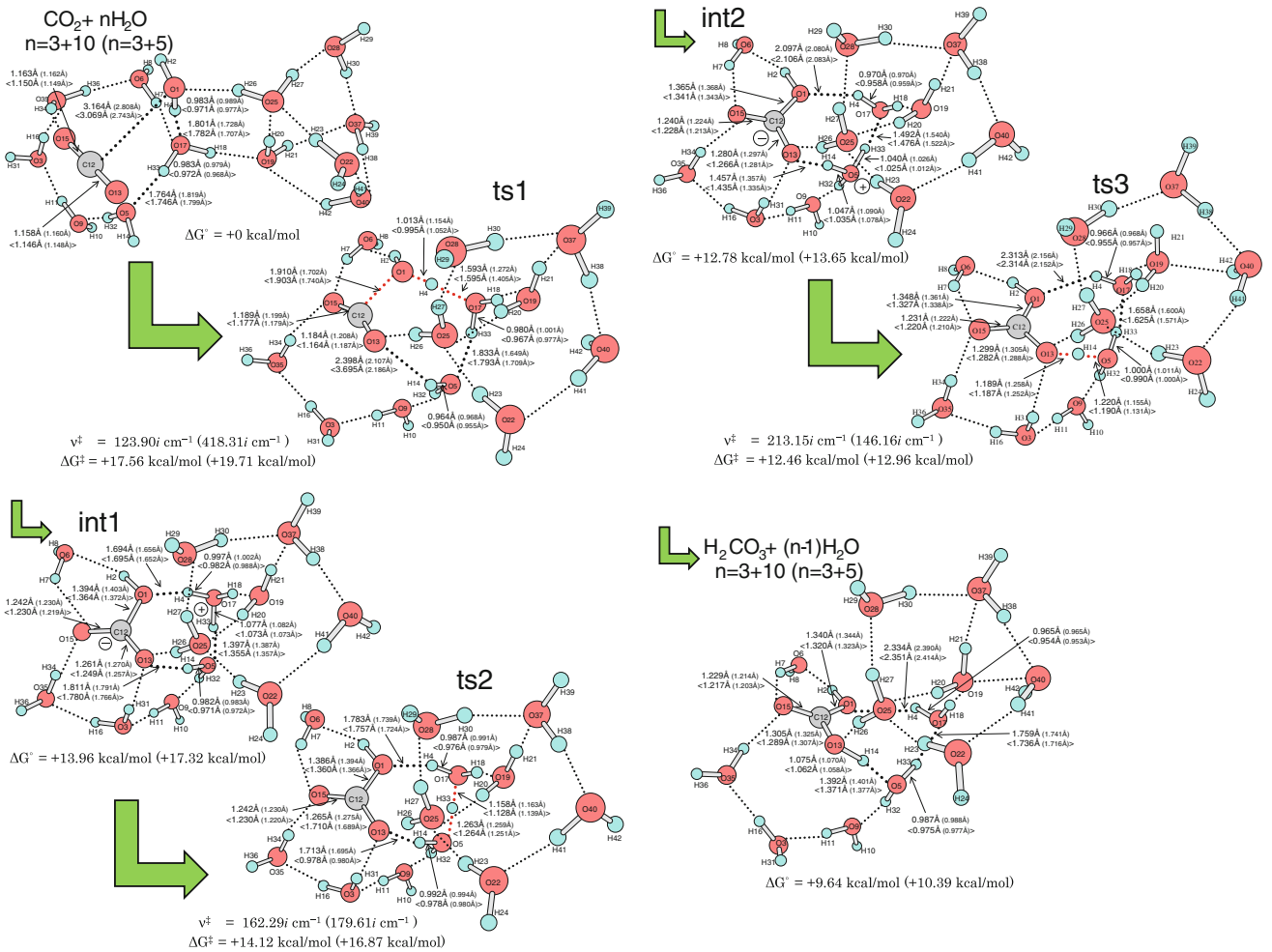

Fig. 4 A stepwise reaction of $CO_2 + nH_2O \rightarrow H_2CO_3 + (n-1)H_2O$ with $n = 3 + 10$ and $(n = 3 + 5)$, where two intermediates, int1 and int2, are involved

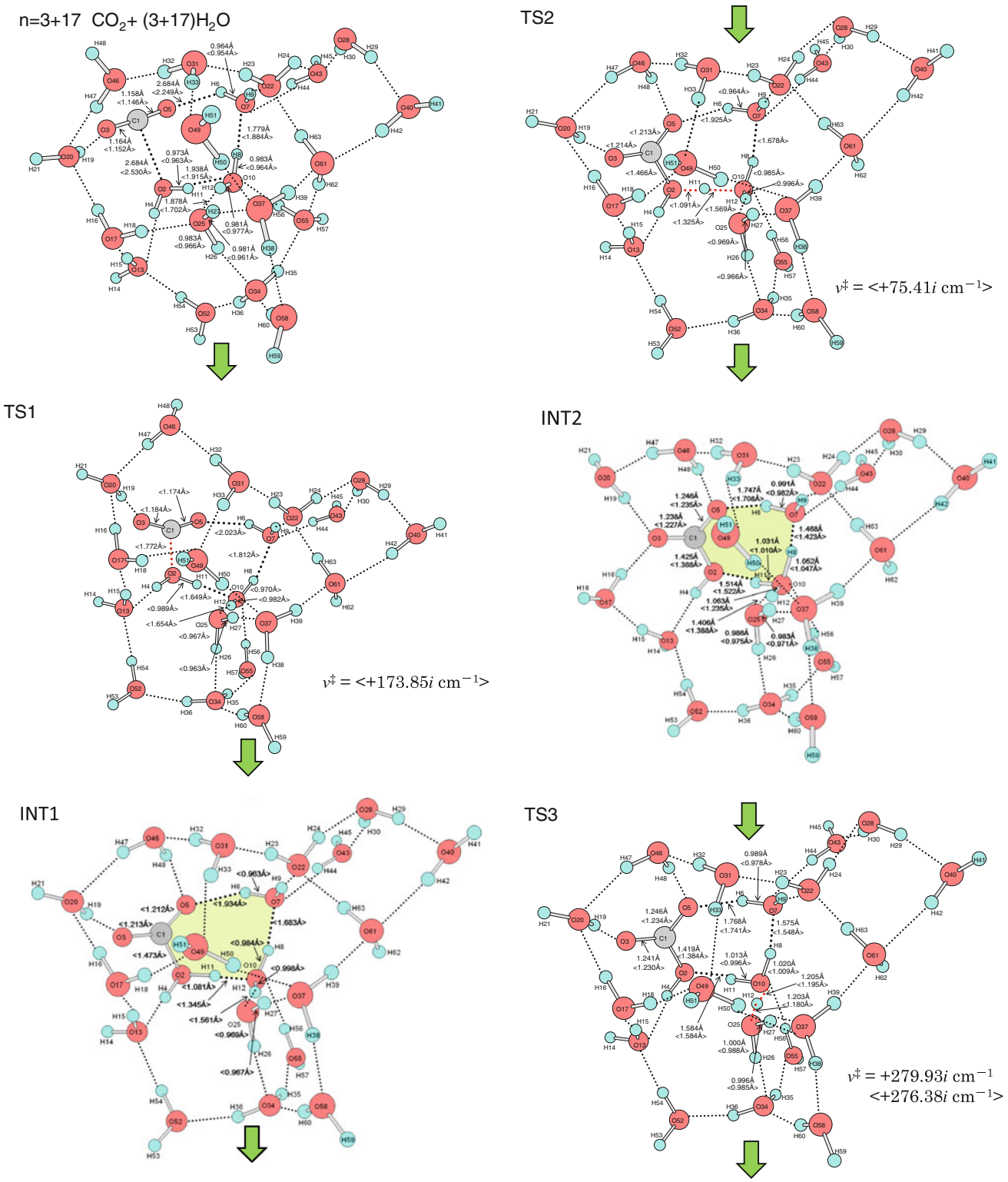

Fig. 5 A stepwise reaction of $CO_2 + (3 + 17)H_2O \rightarrow H_2CO_3 + (2 + 17)H_2O$, where three intermediates, INT1, INT2, and INT3, are involved. The *yellow area* denotes the circuit for bond interchanges and contains $HCO_3^- \cdot H_3O^+$ ion pairs in INT1 and INT2. INT1 and concomitant TS1 and TS2 were not found by B3LYP

They are shown in Scheme 4a and b, respectively. From the Zundel cation, the proton transfer outward is possible leading to the electrolytic dissociation.

Figure 6 shows TS geometries of a reaction of $n = 3 + 27$. Other geometries such as INT1 and INT2 are shown in Figure S1 of Supporting Information. After TS1,

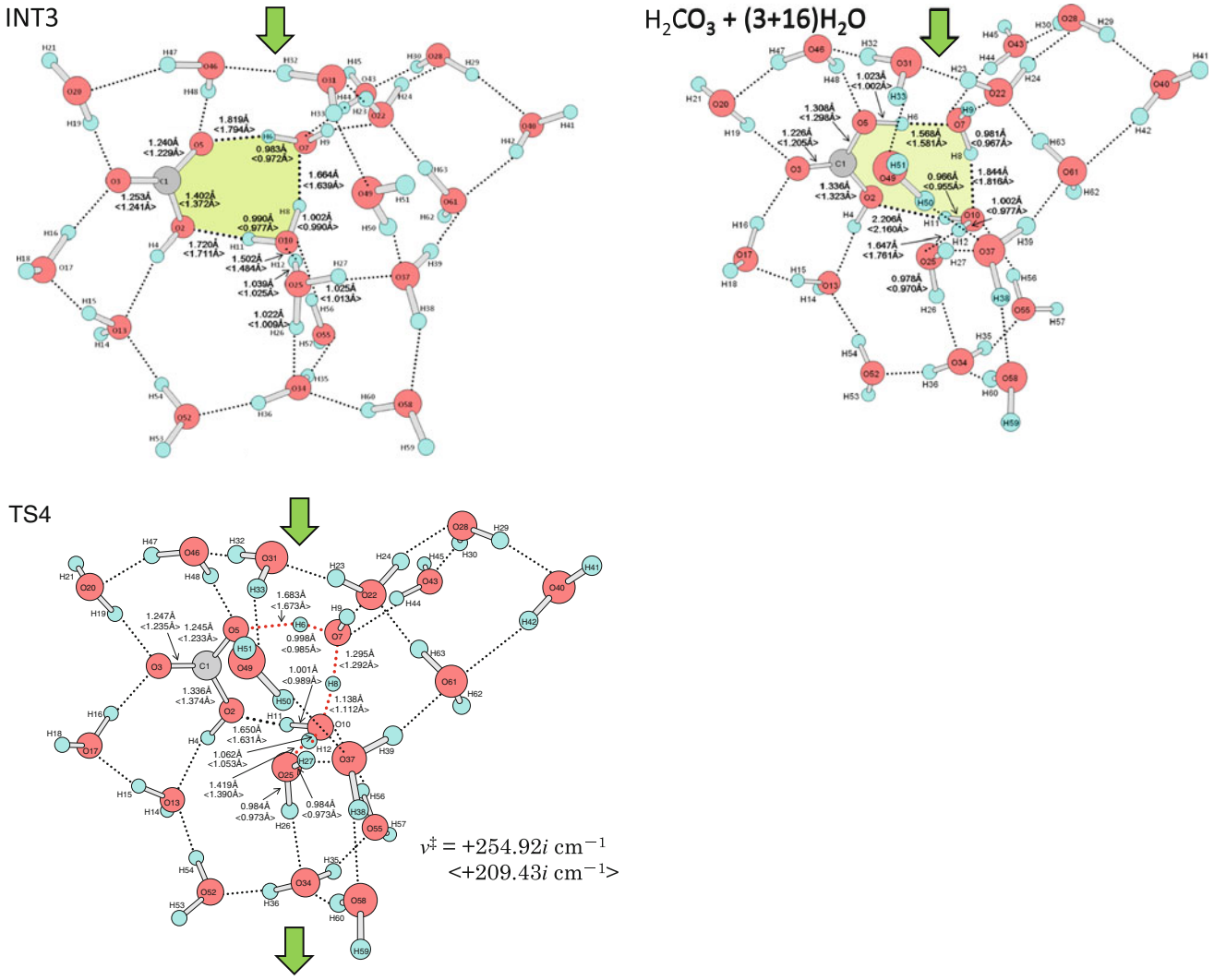

Fig. 5 continued

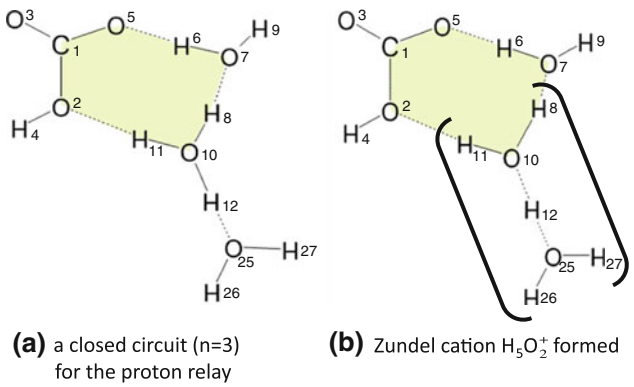

Scheme 4 Two characteristics derived from the $n = 3 + 17$ calculations

a transient intermediate INT1 is afforded. INT1 is isomerized via TS2 to one isomer of the Zundel cation INT2. The other one is INT3 brought about by TS3. From INT2, another isomerization (TS4) leads to H_2CO_3. Thus, the $n = 3 + 27$ model (Fig. 6) gives a result similar to that of $n = 3 + 17$ (Fig. 5).

Figure 7 exhibits changes of B3LYP/6-311+G** SCRF = PCM//B3LYP/6-311+G** Gibbs free energies that correspond to geometric ones of Fig. 6. The rate-determining step is TS1. Three calculated $\Delta G^{\ddagger}$ values are fortuitously in good agreement with experimental data. However, those of MPW1 K/6-311+G** SCRF = PCM//MPW1K/6-311+G** are somewhat underestimated. The stability order is $CO_2 + H_2O > H_2CO_3 > HCO_3^- + H3O^+$. In the

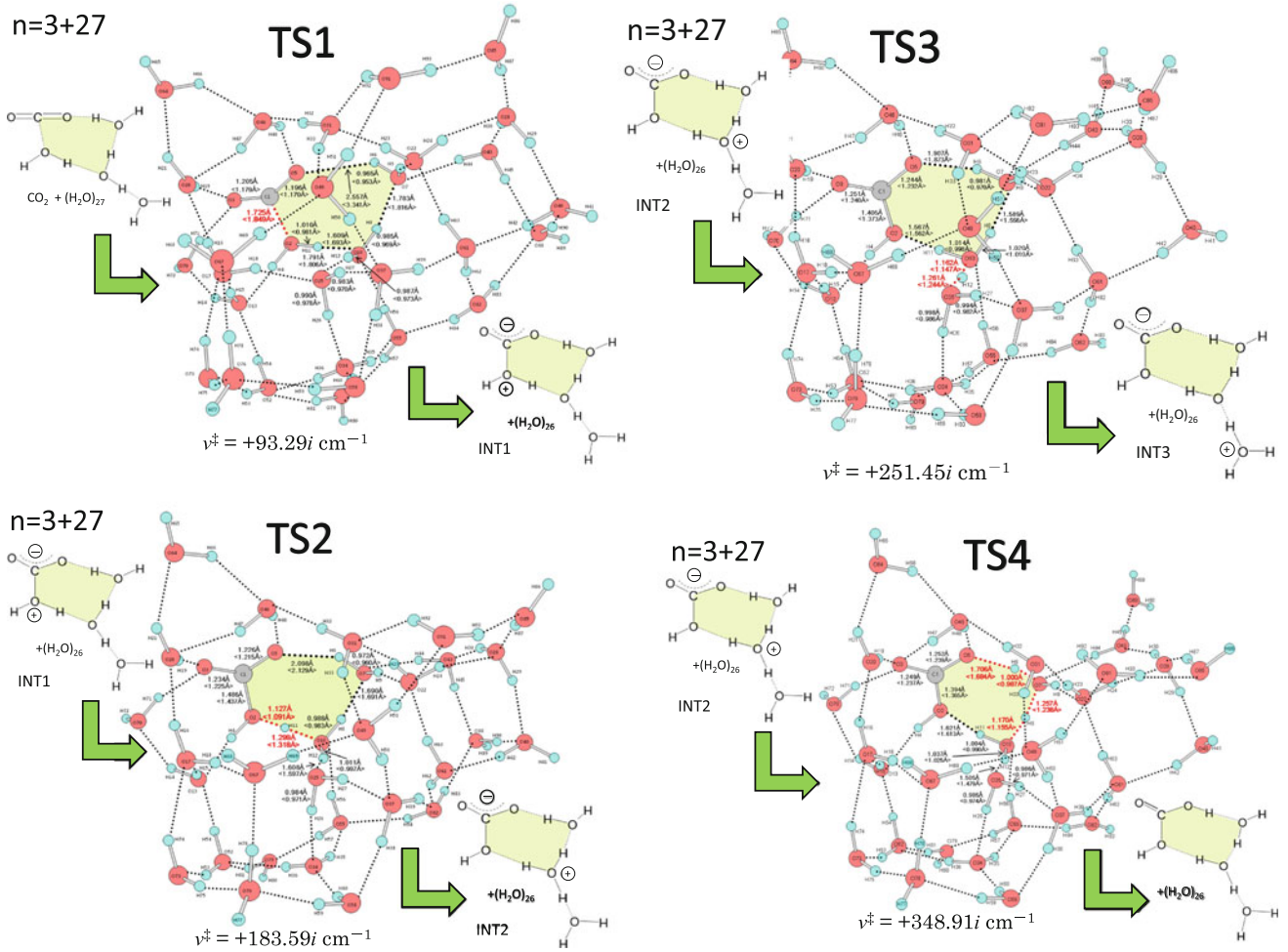

Fig. 6 A stepwise reaction of $CO_2 + (3 + 27)H_2O \rightarrow H_2CO_3 + (2 + 27)H_2O$, where three intermediates, INT1, INT2, and INT3, are involved. Geometries of $CO_2(H_2O)27$, $H_2CO_3(H_2O)26$, INT1, INT2, and INT3 are shown in Figure S1 (Supporting Information)

Zundel cation, INT3 was computed to be much more stable than INT2. While INT3 is a channel for the proton dispersal, its character is retained in the Zundel cation (see Figure S2). It appears to be strange that the energy of TS3 is lower than INT2. This comes from the single-point calculation, B3LYP/6-311+G** SCRF = PCM//B3LYP/6-311+G**. TS3 is the isomerization TS inside the Zundel cation, and the energy barrier is very small to give the strange result. The tunnel effect on the activation energy was examined for TS4 in Fig. 6 which has the largest $|\nu^{\ddagger}|$ value among $n = 3 + 17$ and $n = 3 + 27$ TSs. The energy lowering was calculated to be small (= 0.125 kcal/mol).

The initial state, $CO_2 + H_2O$, is the most stable, where the CO_2 molecule is outside the water cluster (Scheme S2 and Figure S3). Even if the CO_2 molecule is put into the central region of the cluster, it is expelled during the geometry optimization. Thus, the CO_2–H_2O interaction is initiated by formation of INT1.

4 Concluding remarks

In this work, the reaction of $CO_2 + nH_2O$ was investigated computationally. While the computed results depend on the value of n, $n = 3 + 17$ and $n = 3 + 27$ models seem to represent a reliable mechanism. Scheme 5 shows a minimal model summarizing the present results. When a CO_2 molecule is thrown into water, it cannot be blended with the water cluster directly. When INT1 is formed, proton transfer is initiated to give an isomer of the Zundel cation INT2. INT2 is quickly converted to INT3. However, INT3 is less stable than H_2CO_3, and accordingly further isomerization INT3 → INT2 → H_2CO_3 is possible.

A question of which $CO_2 + H_2O \rightarrow H_2CO_3 \rightarrow H^+ + HCO_3^-$ or $CO_2 + H_2O \rightarrow H^+ + HCO_3^- \rightarrow H_2CO_3$ is likely was raised in Scheme S1. Scheme 5 has shown that the latter path is more likely.

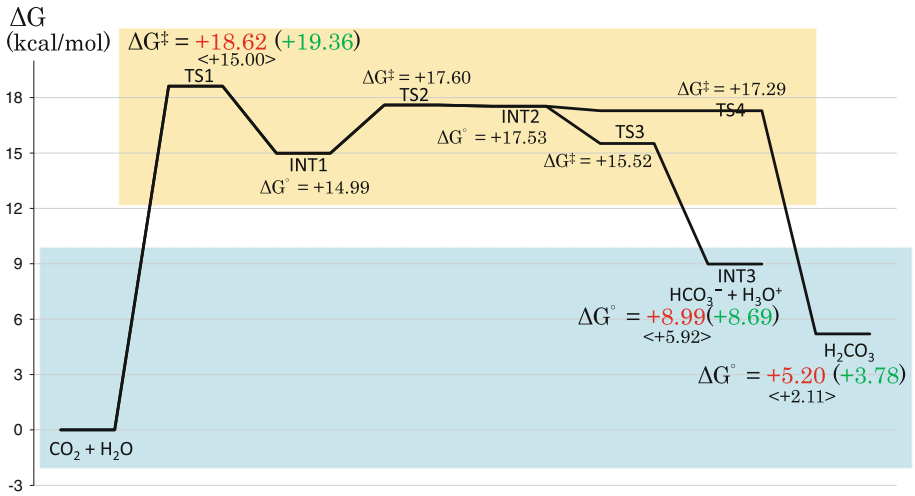

Fig. 7 Changes of Gibbs free energies (in kcal/mol, $T = 298.15$ K, $P = 1$ atm) for the model of $CO_2 + (3 + 27)H_2O$ in Fig. 6 and Figure S1. For TS1, INT3, and H2CO3, <MPW1K/6-311+G(d, p) SCRF = PCM//MPW1K/6-311+G(d, p)> values are also shown.(#3-Q-6) In parentheses, experimental values are shown. Refs. [1, 2] The $\Delta G^{\ddagger}$ changes of two steps, INT2 → TS3 → INT3 and INT2 → TS4 → H_2CO_3, are barrierless, which comes from addition of the B3LYP/6-311+G(d, p) SCRF = PCM single-point electronic energy and the B3LYP/6-311+G(d, p) thermal correction of the Gibbs free energy. Electronic energies of the gas-phase (i.e., in the geometry optimization) are, −2,482.893232 a.u. (INT2), −2,482.893734 a.u. (TS3), −2,482.881457 a.u. (INT3), −2,482.892304 a.u. (TS4), −2,482.912120 a.u. (H_2CO_3)

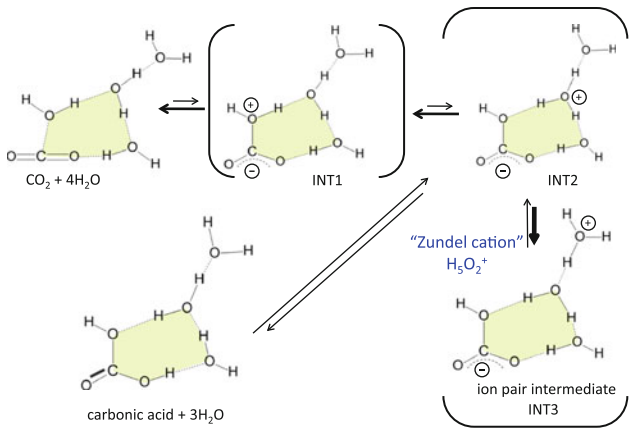

Scheme 5 A minimal model representing the formation and electrolytic dissociation of carbonic acid

Acknowledgments The authors appreciate careful English corrections of one referee for the better presentation of our work.

References

The reference 39 is included in the journal which is now out of print. Therefore, the original reference is shown at the end of Supporting Information under permission of Oldenbourg Verlag.

1. Welch MJ, Lipton JF, Seck JA (1969) J Phys Chem 73:3351
2. Wagman DD, Evans WH, Parker VB, Schumm RH, Halow I, Bailey SM, Churney KL, Nuttal RL (1982) The NBS tables of chemical thermodynamics properties: selected values for inorganic and C1 and C2 organic substances in SI units. J Phys Chem Ref Data 11(Suppl 2):2–392
3. Jonsson B, Karlstrom G, Roos B (1976) Chem Phys Lett 41:317
4. Jonsson B, Karlstrom G, Wennerstrom H, Forsen S, Roos B, Almlof J (1977) J Am Chem Soc 99:4628
5. Nguyen MT, Ha T (1984) J Am Chem Soc 106:599
6. Merz KM Jr (1990) J Am Chem Soc 112:7973
7. Nguyen MT, Raspoet G, Vanquickenborne LG, Duijnen PTV (1997) J Phys Chem A 101:7379
8. Loerting T, Tautermann C, Kroemer RT, Kohl I, Hallbrucker A, Mayer E, Liedl KR (2000) Angew Chem Int Ed 39:891
9. Tautermann CS, Voegele AF, Loerting T, Kohl I, Hallbrucker A, Mayer E, Liedl KR (2002) Chem Eur J 8:66
10. Nguyen MT, Matus MH, Jackson VE, Ngan VT, Rustad JR, Dixon DA (2008) J Phys Chem A 112:10386
11. Deng Z, Polavarapu PL, Ford SJ, Hecht L, Barron LD, Ewig CS, Jalkanen KJ (1996) J Phys Chem 100:2025
12. Jalkanen KJ, Suhai S (1996) Chem Phys 208:81
13. Han WG, Jalkanen KJ, Elstner M, Suhai S (1998) J Phys Chem B 102:2587
14. Jalkanen KJ, Elstner M, Suhai S (2004) J Mol Struct (Theochem) 675:61
15. Bohr H, Jalkanen KJ (2005) In: Clark JW, Panoff RM, Li H (eds) Condensed matter theory, vol 20. Nova Science Publishers, Hauppauge, p 375
16. Jalkanen KJ, Degtyarenko IM, Nieminen RM, Cao X, Nafie LA, Zhu F, Barron LD (2008) Theor Chem Acc 119:191
17. Weise CF, Weisshaar JC (2003) J Phys Chem B 107:3265
18. Poon CD, Samulski ET, Weise CF, Weisshaar JC (2000) J Am Chem Soc 122:5642
19. Mukhopadhyay P, Zuber G, Beratan DN (2008) Biophys J 95:5574
20. Tajkhorshid E, Jalkanen KJ, Suhai S (1998) J Phys Chem B 102:5899

21. Frimand K, Bohr H, Jalkanen KJ, Suhai S (2000) Chem Phys 255:165
22. Jalkanen KJ, Nieminen RM, Frimand K, Bohr J, Bohr H, Wade RC, Tajkhorshid E, Suhai S (2001) Chem Phys 265:125
23. Jalkanen KJ, Jurgensen VW, Claussen A, Jensen GM, Rahim A, Wade RC, Nardi F, Jung C, Nieminen RM, Degtyarenko IM, Herrmann F, Knapp-Mohammady M, Niehaus T, Frimand K, Suhai S (2006) Int J Quantum Chem 106:1160
24. Degtyarenko IM, Jalkanen KJ, Gurtovenko AA, Nieminen RM (2007) J Phys Chem B 111:4227
25. Degtyarenko I, Gurtovenko AA, Jalkanen KJ and Nieminen RM (2008) J Comput Theor Nanosci 5:277–285
26. Deplazes E, Bronswijk WV, Zhu F, Barron LD, Ma S, Nafie LA, Jalkanen KJ (2008) Theor Chem Acc 119:155
27. Losada M, Xu Y (2007) Chem Phys 9:3127
28. Becke AD (1993) J Chem Phys 98:5648
29. Lee C, Yang W, Parr RG (1988) Phys Rev B 37:785
30. Zhao Y, Truhlar DG (2004) J Phys Chem A 108:6908
31. Lynch BJ, Fast PL, Harris M, Truhlar DG (2000) J Phys Chem A 104:4811
32. Moeller C, Plesset MS (1934) Phys Rev 46:618
33. Fukui K (1970) J Phys Chem 74:4161
34. Gonzalez C, Schlegel HB (1989) J Chem Phys 90:2154
35. Cancès E, Mennucci B, Tomasi J (1997) J Chem Phys 107:3032
36. Cossi M, Barone V, Mennucci B, Tomasi J (1998) J Chem Phys Lett 286:253
37. Mennucci B, Tomasi J (1997) J Chem Phys 106:5151
38. Zhao Y, Truhlar DG (2008) Theor Chem Acc 120:215
39. Wigner E (1932) Z Phys Chem B 19:203
40. Mueller EM, de Meijere A, Grubmueller H (2002) J Chem Phys 116:897
41. Gaussian 09, Revision A. 1, Frisch MJ, Trucks GW, Schlegel HB, Scuseria GE, Robb MA, Cheeseman JR, Scalmani G, Barone V, Mennucci B, Petersson GA, Nakatsuji H, Caricato M, Li X, Hratchian HP, Izmaylov AF, Bloino J, Zheng G, Sonnenberg JL, Hada M, Ehara M, Toyota K, Fukuda R, Hasegawa J, Ishida M, Nakajima T, Honda Y, Kitao O, Nakai H, Vreven T, Montgomery Jr. JA, Peralta JE, Ogliaro F, Bearpark M, Heyd JJ, Brothers E, Kudin KN, Staroverov VN, Kobayashi R, Normand J, Raghavachari K, Rendell A, Burant JC, Iyengar SS, Tomasi J, Cossi M, Rega N, Millam NJ, Klene M, Knox JE, Cross JB, Bakken V, Adamo C, Jaramillo J, Gomperts R, Stratmann RE, Yazyev O, Austin AJ, Cammi R, Pomelli C, Ochterski JW, Martin RL, Morokuma K, Zakrzewski VG, Voth GA, Salvador P, Dannenberg JJ, Dapprich S, Daniels AD, Farkas O, Foresman JB, Ortiz JV, Cioslowski J, Fox DJ (2009) Gaussian, Inc., Wallingford
42. Schuster P, Zundel G, Sandorfy C (1976) The hydrogen bond, recent developments in theory and experiments. Amsterdam, North Holland, p 687